Journal of Materials Chemistry A

Accepted Manuscript

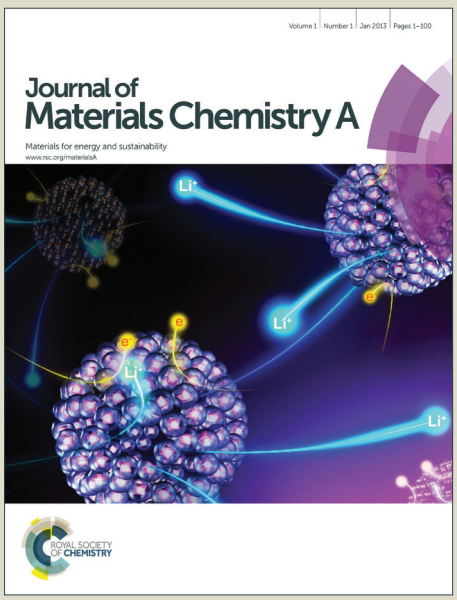

This is an *Accepted Manuscript*, which has been through the Royal Society of Chemistry peer review process and has been accepted for publication.

Accepted Manuscripts are published online shortly after acceptance, before technical editing, formatting and proof reading. Using this free service, authors can make their results available to the community, in citable form, before we publish the edited article. We will replace this *Accepted Manuscript* with the edited and formatted *Advance Article* as soon as it is available.

You can find more information about *Accepted Manuscripts* in the Information for Authors.

Please note that technical editing may introduce minor changes to the text and/or graphics, which may alter content. The journal's standard Terms & Conditions and the Ethical guidelines still apply. In no event shall the Royal Society of Chemistry be held responsible for any errors or omissions in this *Accepted Manuscript* or any consequences arising from the use of any information it contains.

ROYAL SOCIETY OF CHEMISTRY

www.rsc.org/materialsA

Journal of Materials Chemistry A

Dynamic Article Links ►

Cite this: DOI: 10.1039/c0xx00000x

PAPER

www.rsc.org/xxxxxx

Low viscosity highly conductive ionic liquid blends for redox active electrolytes in efficient dye-sensitized solar cells

Maria Bidikoudi,[a] Lawien F. Zubeir,[b] and Polycarpos Falaras*[a]

[a]Division of Physical Chemistry, Institute of Advanced Materials, Physicochemical Processes, Nanotechnology and Microsystems (IAMPPNM), National Center for Scientific Research "Demokritos", 153 10 Agia Paraskevi Attikis, Athens, Greece.
E-mail: papi@chem.demokritos.gr (PF); Fax: +30-2106511766; Tel: +30-2106503644
[b]Dept. Chemical Engineering and Chemistry, Eindhoven University of Technology, Den Dolech 2, 5612 AZ, P.O. Box 513, STO 1.21, 5600 MB Eindhoven, The Netherlands

Received (in XXX, XXX) Xth XXXXXXXXX 200X, Accepted Xth XXXXXXXXX 200X
DOI: 10.1039/b000000x

ABSTRACT

Mixtures of ionic liquids were prepared and used for the development of composite redox electrolytes electrolytes by blending a standard low viscosity ionic liquid solvent (EMimDCA, 1-ethyl-3methylimidazolium dicyanamide) with various iodide-based ionic liquids based on the methylimidazolium cation (DMII, EMII, PMII, BMII and HMII). The novel electrolytes based on the [CnC_1im]I/EMimDCA double salt ILs show interesting physicochemical properties including low viscosity (10-110 MPa s) and high diffusion coefficient of triiodides (DI_3^-, 5-10 × 10^{-7} cm^2/s), respectively, characteristics that promiss increased performance in DSC devices. Their electrochemical properties along with the conductivity were also tuned and optimized; values as high as and 2-4 mS/cm were estimated for the conductivity. Solar cells based on these composite electrolytes attained efficiencies over 4% under 1 sun with the highest being 5.5%, attained by EMimDCA-DMII mixture. Quite notably, these efficiencies further increased up to 6.5%, when the cells were illuminated by 0.1 sun.

1. Introduction

Dye-sensitized solar cells (DSCs) are third generation photovoltaics that have attracted a great deal of attention since the pioneer work of O'Regan and Gratzel reported in Nature[1], due to their low production cost, simple fabrication process and high efficiency[2,3]. A DSC consists primarily of a mesoporous nanocrystalline large band gap semiconducting oxide (sensitized by a molecular dye) photoanode, a redox active electrolyte and a platinum counter electrode. Being a key component of the DSC, the electrolyte has important impact on the operation, performance and stability of DSC. It mainly comprises a redox couple (and eventually some additives) in an appropriate medium, usually a liquid solvent. The mediator regenerates the oxidized dye and its potential determines the maximum cell photovoltage. The solvent insures the structuring of the corresponding interfaces (including the necessary good wetting and passivation of the photoelectrode)[4] and the solubility and transport of the redox active species.

Liquid electrolytes containing the iodine/triiodide (I^-/I_3^-) redox couple in a high dielectric constant organic solvent are frequently used in well performing DSCs. The highest power conversion efficiency attained so far in DSCs incorporating the I^-/I_3^- redox shuttle, is of the order of 12%[5a] in a system incorporating the organic solvents acetonitrile and valeronitrile in the electrolyte, while recently the use of the Co(II)/Co(III) mediator in acetonitrile in a cell based on a porphyrin dye (SM315) has led to efficiency values as high as 13%[5b]. However, liquid DSC devices usually suffer from solvent evaporation as well as concomitant components instability that limit their long-term operation. These problems restrain the large scale application of DSCs and have led the scientific community into exploring to replace the volatile organic solvent used in the electrolyte. Low viscosity ionic liquids (ILs) were revealed as an ideal alternative to overcome the main drawbacks of organic solvent-based electrolytes. Ionic liquids (ILs) are purely ionic, salt-like materials, which are per definition liquid below 100°C. Commonly, they have melting points below room temperature, with some even below 0°C. Room temperature ILs are formed by organic salts containing cations and anions from the halide or pseudo halide family and non-coordinating ions. The increasing interest in ILs largely stems from their green character and unique properties, such as high chemical, electrochemical and thermal stabilities, very low or even negligible vapour pressure, non-flammability, tunable viscosity, solvent ability and high ionic conductivity[6-10]. They were first used in DSCs in Grätzel's laboratory with the primary aim of reducing electrolytes' volatility while preventing voltage drop at the same time, since the IL cations can replace the absorption sites on the TiO_2 surface[11-15]. Ionic liquids with various cations, such as sulfonium, guanidinium, ammonium, phosphonium, pyridinium, pyrrolidinium, piperidinium, have been explored and used as electrolytes for DSCs[16,17] but the ionic liquids that prevailed in use as electrolytes for dye sensitized solar cells are the ones carrying the imidazolium cation, owing to their higher conductivity and lower viscosity[18-20], and the iodide anion, which serves as the source of I^- required for the reduction of the oxidized dye molecules [21].

Among all the room temperature ionic liquid iodide imidazolium salt 1-propyl-3-methyl imidazolium iodide (PMII) presents the lowest viscosity (1024 cP, Table 1) and highest conductivity (0.54 mS/cm) at room temperature and has for this reason been widely used in DSCs with ionic liquid electrolytes, while optimum results have been obtained with the use of iodide eutectic melts [22]. However, it is still

Journal of Materials Chemistry A Accepted Manuscript

viscous enough that the resulting electrolytes lack fluidity, making it difficult for ions to diffuse and causing recombination of electrons. By lowering the viscosity of the binary IL electrolyte there is a simultaneous facilitation of the diffusion of the redox couple within the electrolyte and retardation of the recombination reaction between the injected electrons in the TiO_2 electrode and triiodide anions in the electrolyte[23]. In order to decrease the viscosity and, at the same time, raise the conductivity of solvent free, ionic liquid based electrolytes, iodide salts are usually mixed with a relatively low-viscosity noniodide ionic liquid to formulate a solvent-free electrolyte for highly efficient DSCs[23-28]. In such a system the resulting "solutions" are quite different from mixtures of molecular solvents and the corresponding physical, thermal, and chemical properties can be finely tuned, allowing improved transport of iodides and optimization of the electrode/electrolyte interfaces[29].

Having these in mind, in a recent paper we proceeded with the synthesis of a series of ILs of the type $[C_nC_1im]TCM$, based on 1-alkyl-3-methylimidazolium cations ($[C_nC_1im]^+$) and tricyanomethanide $[C(CN3)^-]$ anions (TCM), where the alkyl chain length was progressively modified by increasing the number of carbon atoms (n = 2, 4, 6, 8). The $[C_nC_1im]TCM$ ionic liquids (viscosity value lowering component) were used upon mixing with 1-propyl-3-methyl imidazolium iodide (PMII-solvent) in the form of blends, in low viscosity solvent free ionic liquid based redox electrolytes. Giving special emphasis to the role of the non-iodine ionic liquid constituent and keeping constant the iodide containing component, the new redox electrolytes were thoroughly characterized and incorporated with success in regenerative DSCs[30].

In this work the above concept was expanded to more advanced ionic liquid mixtures (double salt ionic liquids), where we kept constant the non-iodine ionic liquid (viscosity lowering agent), focusing on the effects of the iodine containing ionic liquid component chain length. We thus developed and systematically examined innovative redox electrolytes based on blends of 1-ethyl-3-methylimidazolium dicyanamide –EMimDCA [a low viscous (21 cP) ionic liquid with a remarkably high conductivity ($\geq 2 \times 10^{-2}$ S x cm^{-1})], with a series of 1-alkyl-3-methylimidazolium iodides $[C_nC_1im]I$ (n = 1, 2, 3, 4, 6)]. The developed electrolytes presented unique properties and were then incorporated in DSCs that were thoroughly characterized in order to establish the dependence of the device efficiency on the cation size of the $[C_nC_1im]I$ electrolyte component. Following the new conceptual approach, the novel electrolytes based on the $[C_nC_1im]I$/EMimDCA double salt ILs show lower viscosity, significantly higher values for the diffusion coefficient of triiodide (D_{I3-}), higher conductivity (κ), lower series (Rs) and charge transfer (Rct) resistances, characteristic properties that justify the increased performance of the corresponding DSC devices.

2. Experimental Section

2.1 Materials

Different 1-alkyl-methylimidazolium iodide-based ionic liquids were purchased from Iolitec. The Z907 dye is a Ru^{2+} based dye, $RuLL'(NCS)_2$ (L=2,2'-bipyridyl-4,4'-dicarboxylic acid; L'=4,4'-dinonyl-2,2'-bipyridine), purchased from Dyesol UK. Transparent fluorine doped tin oxide (FTO) conductive glass substrates were obtained by Pilkington (8 Ohm/square). Ti Nanoxide D/SP paste, containing small (15-20 nm) and larger diffusing particles (100 nm), was purchased from Solaronix, Switzerland. $TiCl_4$ was bought from Fluka.

2.2 Redox electrolytes

Ionic liquid based electrolytes consisting of 0.1 M LiI and 0.2 M I_2 were prepared by dissolving the redox couple in a blend of EMimDCA/ $[C_nC_1im]I$ [EMimDCA= 1-ethyl-3-methylimidazolium dicyanamide and $[C_nC_1im]I$ = 1-alkyl-3-methylimidazolium iodide (n = 1, 2, 3, 4, 6)], in a 7:13 v/v proportion. 0.4 M 4-tert-butyl pyridine (4-TBP) was also added in the final mixture in order to increase the photovoltaic efficiencies[31]. For simplicity reasons, the above electrolytes will be referred as C1, C2, C3, C4 and C6 according to the above compositions, in both text and Tables.

2.3 Electrodes and solar cells fabrication

To construct the photoelectrodes, opaque TiO_2 films (about 5.5-6 μm thick, determined by an AMBIOS XP-2 profilometer) were deposited by doctor-blading the TiO_2 paste (Ti Nanoxide D/SP) on transparent conductive glass substrates and sintered at 125 (5 min), 325 (15 min) and 525 ^{0}C for 30 min in air (heating rate: 5 ^{0}C min^{-1}). Afterwards, the films were post-treated with an aqueous solution of 40 mM $TiCl_4$ for 30 min at 70 ^{0}C. Subsequently, they were thoroughly cleaned with de-ionized water and ethanol and left to dry in air. Finally, the films were heated once again at 450 ^{0}C for 60 min and further sensitized by their immersion in a 0.3 mM solution of Z907 dye in acetonitrile/tert-butanol (1:1 v/v) containing equal moles of chenodeoxycholic acid. Pt counter electrodes (100 nm thick) were prepared by sputtering. Open (non-sealed) DSCs were fabricated by putting a small drop of the electrolytes onto the sensitized photoelectrode and simply sandwiching the counter electrode against the first electrode. All DSCs had an active area of 0.25 cm^2 and were tested one hour after their preparation.

2.4 Characterization techniques and instrumentation

The density and the viscosity of the electrolytes were determined at atmospheric pressure and at temperatures ranging from 288 to 368 K. Due to the high hygroscopicity of the samples, both properties were measured using an Anton Paar SVM 3000/G2 Stabinger viscometer provided with a high-precision thermostat with stability of 0.005 K and calibrated by the manufacturer. The uncertainties of density (with viscosity correction) and viscosity measurements are ±0.0005 g cm^{-3} and 0.35% respectively. The equipment requires only a total volume of sample of 2.5 ml for the determination of both the properties and a lack of contact with the open atmosphere avoids moisture capture from air.

Journal of Materials Chemistry A Accepted Manuscript

CREATED USING THE RSC ARTICLE TEMPLATE (VER. 3.1) - SEE WWW.RSC.ORG/ELECTRONICFILES FOR DETAILS

Linear sweep voltammograms (LSV) were recorded on thin layer symmetrical cells made of identical Pt blocking electrodes (prepared by sputtering) by filling them with the electrolytes. LSV experiments were conducted using an Autolab PGSTAT-30 potentiostat (Ecochemie) with a scan rate of 20 mV sec^{-1} and a voltage range from -0.7 to +0.7 vs. Pt. Electrochemical impedance spectra (EIS) were recorded on the above cells using the same potentiostat, equipped with a frequency response analyzer (FRA), at 0 V vs. Pt in the dark and recorded over a frequency range of 100 kHz to 10 mHz. In order to accurately determine the conductivity cell constant, a calibration was carried out using a standard solution (10 mM of KCl in water) with known conductivity (1413 μS cm^{-1}). The obtained spectra were fitted with the FRA software provided by the Autolab in terms of appropriate equivalent circuits.

Current-voltage (I-V) measurements were performed by illuminating the DSCs using solar simulated light (1 sun, 1000 W m^{-2}) from a 300W-Xe source (Oriel) in combination with AM 1.5G optical filter. The active area of the DSCs was set at 0.15 cm^2, using a large black mask in front of the cells in order to avoid any light pipping inside the cell [32]. The J-V characteristics were recorded using linear sweep voltammetry on the Autolab potentiostat working in a 2-electrode mode at a scan rate of 50 mV s^{-1}. EIS measurements on complete DSCs were performed under dark in a potential window from 0 to -0.8 V. Photoelectrochemical and photovoltaic characterization was performed on a batch of at least three DSCs for each electrolyte, and the mean value (without a significant deviation) for the obtained results was derived. Results from electrochemical and photoelectrochemical measurements were deduced from the cells that presented performance close to the average.

3. Results and discussion

3.1 Physicochemical, transport and electrochemical properties of the redox electrolytes

The physicochemical properties of ionic liquids (ILs) can be fine-tuned by the independent selection of cations and anions. This conceptual approach can be further exploited by using mixtures of ionic liquids (Table 1), where the product is a completely new ionic liquid[33].

Table 1. Structure and viscosity of the $[C_nC_1im]X$ ILs and EMimDCA used for the preparation of composite redox electrolytes

Name $[C_nC_1im]X$	Abbreviation	Molecular Formula	Chemical Structure	Viscosity(cP) at 25º C
1,3-Dimethylimidazolium iodide	DMII $[C_1C_1im]I$	$C_5H_9N_2I$		Solid
1-ethyl-3-methylimidazolium iodide	EMII $[C_2C_1im]I$	$C_6H_{11}N_2I$	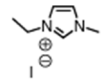	Solid
1-propyl-3-methylimidazolium iodide	PMII $[C_3C_1im]I$	$C_7H_{13}N_2I$	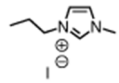	1024[34]
1-butyl-3-methylimidazolium iodide	BMII $[C_4C_1im]I$	$C_8H_{15}N_2I$	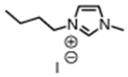	1110[35]
1-hexyl-3-methylimidazolium iodide	HMII $[C_6C_1im]I$	$C_{10}H_{19}N_2I$	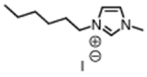	1800[36]
1-ethyl-3-methylimidazolium dicyanamide	EMimDCA $[C_2C_1im]DCA$	$C_8H_{11}N_5$		21[37]

The $[C_nC_1im]I$ ionic liquids were mixed with EMimDCA (low viscosity solvent, Table 1) in a standard 13:7 v/v ratio and the resulting blends (double salt ionic liquids) were used to prepare redox electrolytes with the addition of LiI, I_2 and 4TBP[38]. The physicochemical and transport properties of the resulting five new electrolytes are necessary for the investigation and optimization of their operation in a dye-sensitized solar cell. The determination of density (ρ) and viscosity (η) of the new redox electrolytes were carried out at atmospheric pressure and at temperatures ranging from 288 to 368 K.

Generally,in a narrow range of temperatures, density ρ (gr cm^{-3}) can be expressed following equation (1):

$$\rho = D_\rho + F_\rho T \qquad (1)$$

where D_ρ ,F_ρ and T are the density at 0 K(gr cm^{-3}), the coefficient of volume expansion (gr cm^{-3} K^{-1}) and temperature (K), respectively. This equation permits to express the density of the electrolytes as a function of temperature and the fitting permitted the calculation of the corresponding parameters D_ρ and F_ρ (summarized in Table 2).

Journal of Materials Chemistry A Accepted Manuscript

Table 2 Parameters (D_ρ and F_ρ) derived from linear fitting of the electrolytes' density dependence on the temperature along with the VTF equation parameters (A, B and C) of viscosity (see the text for details) for the same system. A=ln(η_0), B=E (E being the activation energy), and C=T_V (where T_V stands for the Vogel temperature)

Electrolyte	A(10^{-1} mPa s)	B(K)	C(K)	D_ρ(g cm^{-3})	F_ρ(10^{-4} g cm^{-3} K^{-1})
C1	-1.64	677.4	180.7	1.71	-7.92
C2	-1.62	686.9	170.1	1.59	-7.54
C3	-1.86	757.9	181.3	1.63	-7.57
C4	-1.95	784.1	176.7	1.58	-7.46
C6	-1.99	820.4	177.2	1.52	-7.22

Both parameters follow the same trend as in the case of the density values , with C1 presenting the highest values, which implies that the binary electrolyte has the denser structure. A strong linear relationship with temperature was obtained for all systems under study,as shown in Figure 1[39].

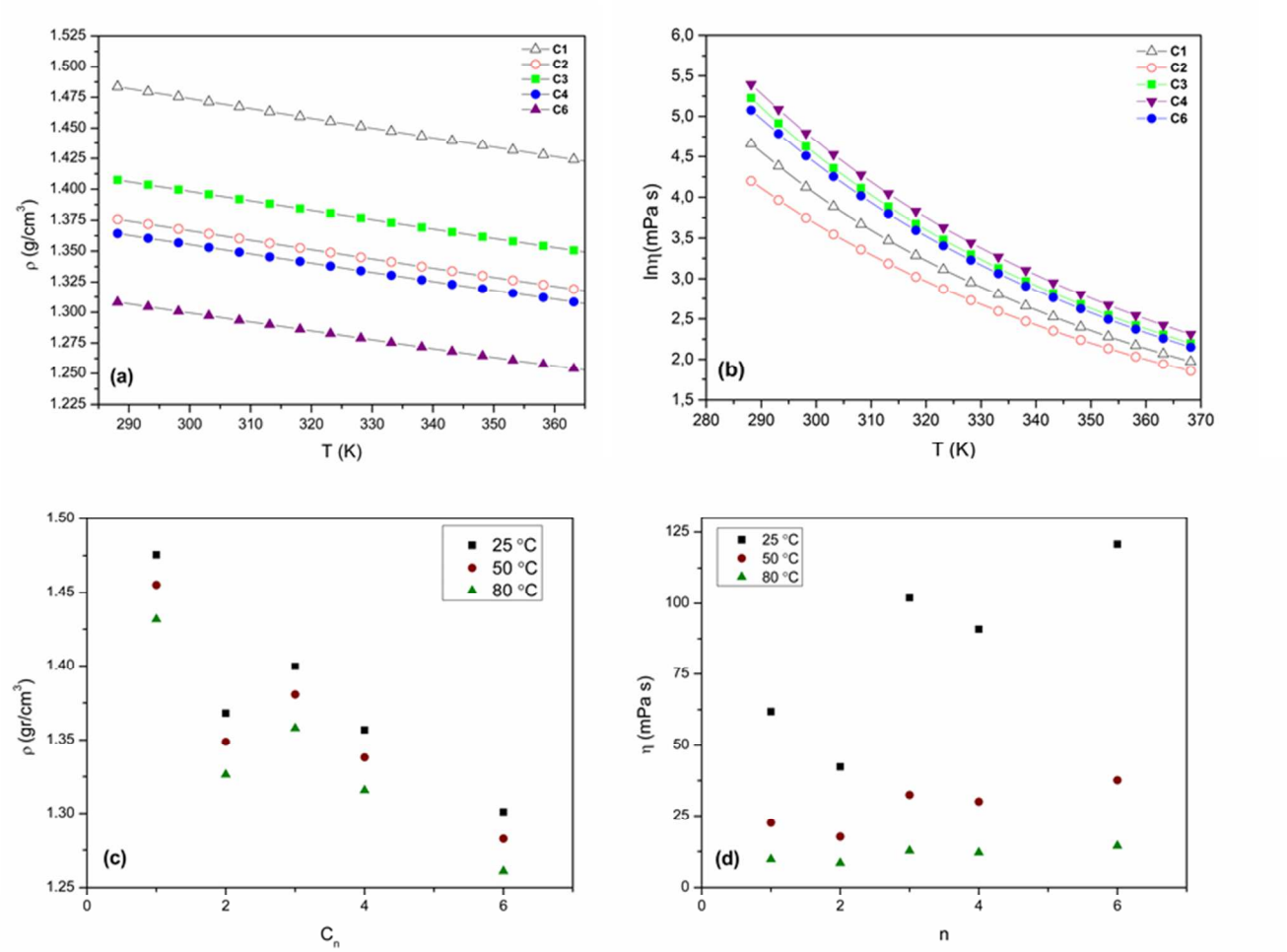

Fig. 1 (a) Temperature dependence of density (a) and viscosity (b) data for the different redox electrolytes based on the [$C_nC_1$im]I/EMimDCA double salt ionic liquids. Plots of their density (c) and viscosity (d) against the number of carbon atoms (n) in the [$C_nC_1$im]I component.

Electrolyte C1 is the one system showing the largest deviation among the results of both density and viscosity. This could be attributed to the solid nature of ionic liquid EMII, which becomes liquid after being blended with a liquid state non iodide ionic liquid, or heating.

The viscosity of an IL is related to the ability of its constituting particles to move in response to an applied force. The viscosity values , η, were fitted using Vogel–Tamman–Fulcher (VTF) equation and modified Vogel–Tamman–Fulcher (modified VTF) equation. The most commonly used equation to correlate the variation of viscosity with temperature is the Arrhenius-like law, but according to Seddon et al. [40] the Arrhenius law can generally be applied when the cation presents only a limited symmetry. If this is not the case, Vogel–Tamman–Fulcher (VTF) and modified equation Vogel–Tamman– Fulcher are recommended[40]. The modified VTF equation can be expressed as:

Journal of Materials Chemistry A Accepted Manuscript

$$\eta = \eta_0 \exp[-E/(T-T_v)] \quad (2)$$

where E is the activation energy and T_V stands for the Vogel temperature. The Vogel temperature (T_v) corresponds to the temperature at which the viscosity is infinite and flow can no longer occur (it is relatively close to the glass transition temperature). When T_V tends to 0, the VTF equation reduces to the simple Arrhenius form. From the analysis and the determination of all parameters, the most important feature is that the electrolyte corresponding to the $[C_1C_1im]I$ constituent in the $[C_nC_1im]I$/EMimDCA blend presents the lowest activation energy (Table 2) with only slight difference from $[C_2C_1im]I$. These two systems also present similar viscosity values, the lowest of all systems studied, explaining the highest overall efficiencies obtained when incorporated in solar cells. When the temperature rises, the thermal agitation, and hence the entropic contribution to the free energy, increase, making the liquid state more stable and the fluidity larger[41a,b]. As a result, temperature rise implies a simultaneous decrease of viscosity (Figure 1). When continuing to raise the temperature above 350 K, all electrolytes tend towards the same value.

Both density and viscosity of the new redox electrolytes based on $[C_nC_1im]I$/EMimDCA blends showed a clear dependence on the number of carbon atoms in the $[C_nC_1im]I$ component, as shown in Figure 1. As a general trend, the decrease of the alkyl chain of the CnC1im constituent results in a net increase of the density and concomitant reduction of the viscosity of the corresponding electrolytes based in the [CnC1im]I/EMimDCA mixtures (no linear behaviour). EMimDCA IL is an excellent solvent for both solid and liquid [CnC1im]I materials, giving electrolytes of low density and moderate viscosity, significantly lower than those based the [CnC1im]TCM//PMII mixtures[30]. Such a relatively low viscosity can effectively alleviate the mass transfer limitations by the contribution of a Grotthus-type charge exchange mechanism[42], affecting both the diffusion coefficient of triiodide (DI3-) and the conductivity (κ) of the electrolyte.

The electrochemical properties of the $[C_nC_1im]I$/EMimDCA blend-based redox electrolytes were investigated in order to determine their conductivity and ionic diffusion properties. These parameters that largely influence the effective behaviour of the electrolytes in a dye-sensitized solar cell were determined in symmetrical cells of the type Pt/electrolyte/Pt, using linear sweep voltammetry (LSV-Figure 2a) and electrochemical impedance spectroscopy (EIS-Figure 2b), and the obtained results are summarized in Table 3.

Initially, the apparent diffusion coefficients (D_{app}) of current-limiting I_3^- species were estimated from the cathodic steady-state currents of the linear sweep voltammograms according to the relation $D_{app}=J_{lim}l/(2nFC)$, where J_{lim} is the limiting current, l is the distance between the two electrodes, F is the Faraday constant, C is the bulk concentration of the diffusion-limiting species and n is the number of electrons transferred in the $I_3^- + 2e^- \rightarrow 3I^-$ redox reaction[43]. The diffusion coefficients vary significantly, displaying values between 3.5 and 10.7×10^7 cm^2 s^{-1}, depending on the binary IL mixture.

It would be expected that, raising the number of atoms in the carbon chain of $C_n$mimI ionic liquid, the I_3^- diffusion coefficient would lower, since such an increase of the chain length would lead to the increase of the ionic liquid electrolyte's viscosity. This trend is obvious when moving from C3 to C4 and C6. However, when moving from C1 to C2 electrolyte, the ones that contain the ionic liquids EMII and DMII, which are in solid state at room temperature, there is a noteable increase of the limiting current J_{lim} and, thus, the I_3^- diffusion coefficient.This result could imply that, when blended with EMimDCA and transitioning at the liquid phase, EMII is less viscous than DMII, even though its alkyl chain is longer. Lower values of viscosity enable the electrolyte to carry increased amount of charge, explaining the higher values of current density obtained when electrolyte C2 is incorporated in solar cells. The above blends did not exhibit a Stokesian behaviour, at least under room temperature, as the values of the Einstein–Stokes ratios of the I_3^- diffusion coefficients ($D_{I3-}\eta/T$) of the blends did not stay constant as anticipated, following the (modified) Stokes-Einstein equation[20]: $D_{I3-}\eta/T=k_B/6\pi r_H$, where k_B is the Boltzmann constant and r_H stands for the effective hydrodynamic radius of triiodide. These results are in full agreement with similar studies in literature[2,44]. This anomalous transport behaviour has been qualitatively explained by the Grotthus-like exchange mechanism, which contributes to the physical ionic diffusion, thus increasing the apparent diffusion coefficients of redox species, despite the relatively large viscosity of the systems

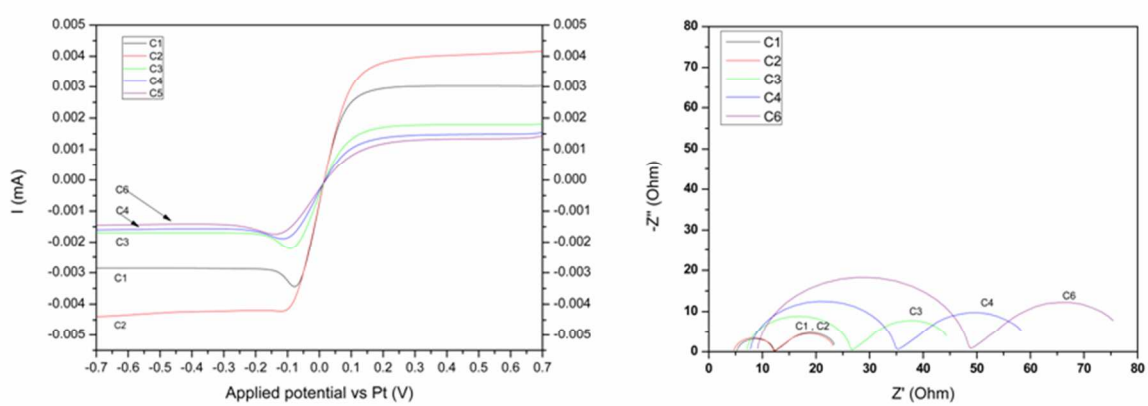

Fig. 2 (a) Linear sweep voltammetry (LSV) measurements on thin symmetrical cells incorporating the redox active electrolytes based on the [CnC1im]I/EMimDCA double salt ionic liquids and (b) Nyquist plots derived by electrochemical Impedance spectroscopy (EIS) spectra using the above symmetrical configuration. For details, see the experimental section.

Journal of Materials Chemistry A Accepted Manuscript

The observed trend in diffusion coefficients was further verified by recording EIS spectra on the same symmetrical cells. The spectra composed of two depressed semicircles (Fig. 2b) attributed to charge transfer at the Pt/electrolyte interface and to the diffusion of ions in the electrolyte, respectively[45]. An electrical equivalent circuit of the type $R_s(C_{dl}[R_{ct}O])$ was used[46], where R_s is the series resistance, R_{ct} and C_{dl} stand for the charge transfer resistance and double layer capacitance at the Pt/electrolyte interface respectively, and O is an element defining the diffusion complex impedance, expressed by the following equation: $Z_{Dif}(\omega)=R_{Dif}\{[\coth(j\omega\tau)^{1/2}]/(j\omega\tau)^{1/2}\}$ with $R_{Dif}=B/Y_o$ and $\tau=B^2$. All the basic parameters, determined by spectral fitting, are summarized in Table 3. The symmetrical cells, comprising the five different electrolytes, differ in the Ohmic resistance values, and since the resistances of the two electrodes (and cables) are identical for all systems, this difference should be reflected at the conductivity of the electrolytes. Using the simple equation $\kappa=1/\rho$ (and $\rho=R_sA/l$)[47], where κ is the specific conductivity, ρ is the resistivity and A is the active area of the cell in cm^2, values of 2 to 3.9 mS cm^{-1} could be estimated, in agreement with relevant values found in literature[48]. The observed trend, i.e. decrease of the specific conductivity upon viscosity increase, with the distinctive singularity of C2 electrolyte, correlates very well with the observed differences in the diffusion coefficients.As reported in previous work (reference to paper mas me to TCM) increasing chain length leads in inrease of both resistances, arising from increased viscosity. A more viscous means hinders the mobility of ions, resulting in slower diffusion.The above results are reflected in the values of diffusion coefficients calculated, as well as in the values of J_s obtained from DSCs fabricated with each electrolyte (see following paragraph). The triiodide diffusion coefficients could be independently determined also using the following equation: $D_{I3^-} = (0.5l/B)^2$. The obtained D_{I3-} were slightly different (3.4 up to about 10.1 × 10^{-7} cm^2 s^{-1}) compared to those determined by linear sweep voltammetry, however, the tendency observed in polarization measurements, was confirmed in this case, too. This feature is not unusual, since similar differences in diffusion coefficients were previously observed, when these are deduced from polarization or impedance spectroscopy measurements on symmetrical cells based on the standard I^-/I_3^- redox couple[49].

Table 3 Electrical parameters (derived by fitting of the EIS spectra), triiodide apparent diffusion coefficient (D_{I3-}) and specific conductivity obtained from EIS measurements for different $[C_nC_1im]I$/EMimDCA based electrolytes (measured at room temperature)

Electrolyte	R_s (Ohm)	R_{ct} (Ohm)	B ($s^{1/2}$)	[a]D_{I3-} (10^{-7} cm^2 s^{-1})	[b]D_{I3-} (10^{-7} cm^2 s^{-1})	κ (mS cm^{-1})
C1	5.40	6.75	2.53	8.68	6.99	3.50
C2	4.85	7.20	2.35	10.09	10.73	3.89
C3	7.20	19.18	3.05	5.98	4.15	2.62
C4	7.82	27.00	3.21	5.40	3.92	2.41
C6	9.15	39.2	3.54	4.46	3.55	2.06

[a]: determind using EIS; [b]: determined using LSV.

Another important issue is the variation of the charge transfer resistance at the electrode/electrolyte interface (R_{ct}) upon changing the ionic liquid electrolyte. It was then found that R_{ct} progressively increased when moving from C1 to C6 electrolyte (Table 3). These findings are in great accordance with the progressive decrease of the fill factor of the DSCs (see following paragraph). In addition, the new electrolytes based on the $[C_nC_1im]I$/EMimDCA double salt ILs present significantly higher values for the diffusion coefficient of triiodides (D_{I3-}), lower series resistance (Rs) and higher specific conductivity (κ) than those based the $[C_nC_1im]$TCM//PMII mixtures[30].

3.2 Photovoltaic performance

The prepared redox electrolytes were incorporated in solar cells using nanoparticulate titania films sensitized with the Z907 dye as photoanodes and their photovoltaic performance was examined. The current-voltage measurements (J-V curves, Figure 3) were obtained by applying a potential scan from 0 V (short-circuit conditions) to the open-circuit potential, under constant 1 sun (AM 1.5G) illumination conditions and under dark and the electrical parameters are included in Table 4.

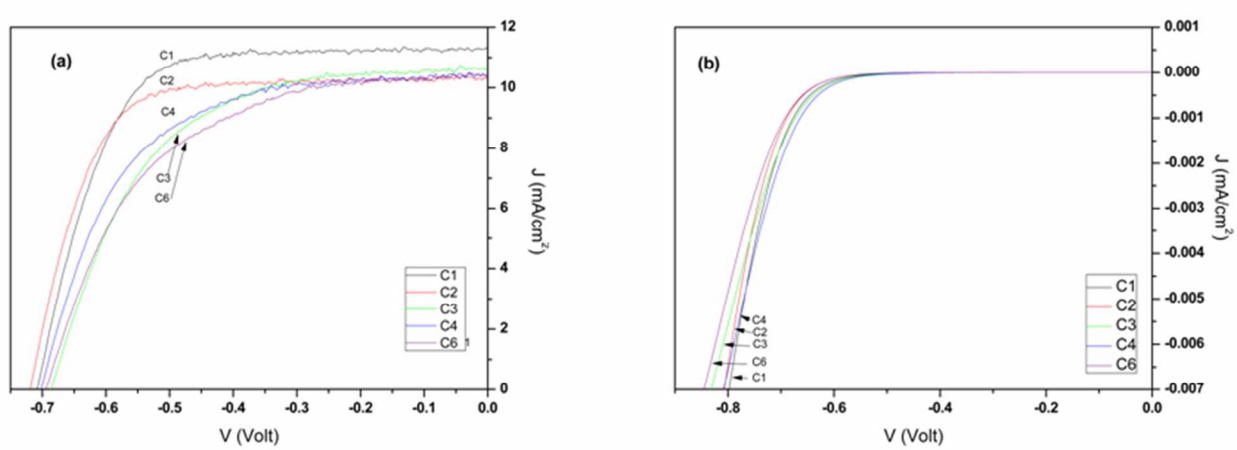

Journal of Materials Chemistry A Accepted Manuscript

Fig. 3 Current density-voltage characteristics under 1 sun AM 1.5G illumination (a) and in dark (b) of optimum DSCs using redox electrolytes based on [$C_nC_1$im]I/EMimDCA double salt ILs.

It must be pointed out that C2-electrolyte, that presented the greatest conductivity and highest diffusion coefficients, attained the highest open circuit voltage (Voc) of 720 mV and highest fill factor (FF) of 0.7 and an overall power conversion efficiency (*PCE*) of 5.27%; however, the photocurrent density (J_{sc}) was lower than the corresponding values of C1-electrolyte. It was then proved that C1 was the most efficient when incorporated in DSCs, attaining overall power conversion efficiencies of over 5,5%. When moving from C1 to C6 electrolyte, one could observe that there is no typical trend followed by the related electrical parameters. There is a noticeable drop of the photocurrent density and the fill factor, which is responsible for the distinctively lower efficiencies attained with electrolytes C3 to C6. A small deviation exists in the case of photovoltage where C1, C2 and C4 electrolytes attained a similar V_{oc} of 702-710 mV while C3 and C6 electrolytes presented a similar photopotential of 691 mV (mean value). The variations observed in V_{oc} for the different electrolytes were further verified by measuring the dark current of the cells (Fig. 3b);

Table 4 Cell parameters derived from J-V curves on DSCs using redox electrolytes based on [$C_nC_1$im]I/EMimDCA double salt ILs, under different levels of light illumination

Electrolyte	Illumination intensity	J_{sc} (mA cm^{-2}) (±0.2 mA cm^{-2})	V_{oc} (V) (±0.01 V)	FF (±0.01)	PCE (%) (±0.2 %)
C1	1 sun	11.26	0.708	0.69	5.53
	0.5 sun	5.80	0.694	0.74	5.97
	0.23 sun	2.90	0.675	0.75	6.39
	0.1 sun	1.32	0.650	0.76	6.56
C2	1 sun	10.39	0.720	0.70	5.27
	0.5 sun	5.36	0.707	0.74	5.58
	0.23 sun	2.64	0.689	0.74	5.89
	0.1 sun	1.21	0.664	0.74	5.94
C3	1 sun	10.66	0.687	0.57	4.17
	0.5 sun	5.60	0.675	0.69	5.21
	0.23 sun	2.77	0.659	0.72	5.70
	0.1 sun	1.29	0.636	0.73	6.00
C4	1 sun	10.39	0.702	0.59	4.32
	0.5 sun	5.43	0.691	0.71	5.33
	0.23 sun	2.72	0.673	0.73	5.78
	0.1 sun	1.24	0.650	0.73	5.88
C6	1 sun	10.42	0.695	0.55	3.97
	0.5 sun	5.62	0.687	0.70	5.45
	0.23 sun	2.84	0.675	0.73	6.10
	0.1 sun	1.29	0.654	0.75	6.34

The corresponding *J-V* curves under different solar light illumination conditions (from 0.5 down to 0.1 sun) were also taken (not shown) and the corresponding electrical parameters are included in Table 4. It was then found that upon decreasing the illumination intensity, the C1 electrolyte increased the efficiency from 5.53% up to 6.56 % at 0.1 sun; accordingly, all the other electrolytes presented similar (increasing) behaviour. It is worth noting that, as the number of carbon atoms increases, efficiency presents a larger deviation when lowering the light intensity. This is more obvious for C6-electrolyte, where efficiency increases by 38% (6.34% from 3.97%)., implying that the electrolyte is able to effectively carry the load in lower light intensity.

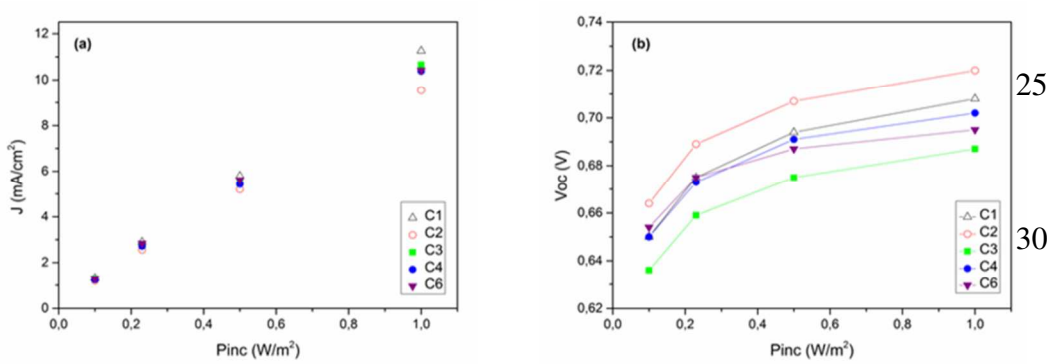

Fig. 4 Linear plots of short circuit photocurrent density (J_{sc}) (a) and open circuit photovoltage (Voc) (b) versus incident power density (Pinc) of optimum DSCs incorporating the redox electrolytes based on [$C_nC_1$im]I/EMimDCA double salt ILs.

Journal of Materials Chemistry A Accepted Manuscript

These phenomena have been frequently observed by others too[50] and have been assigned to restricted diffusion of the ions under strong light illumination, i.e. conditions where the dye injects a lot of electrons and needs a lot of iodide for efficient regeneration[51]. Limited mass transport was further verified by plotting the photocurrent against the incident power density; all electrolytes presented a deviation from perfect linearity (Figure 4). It should be noted, at this point, that the higher the incident power density, the higher the temperature under which the cell is operating. This temperature increase reduces the viscosity of electrolytes, diminishing the diffusion resistance and increasing the diffusion coefficient[52]. However, as one can see from Figure 4b, at higher light intensities (> 0,23 sun) lineariy is lost, implying severe losses caused by recombination through the back contact[53]. In any event, we should highlight that our ionic liquid electrolytes could effectively work under low light conditions, by carrying the charges more easily between the two electrodes, attaining efficiencies of 5.9-6.6% under 0.1 sun.

3.3 Solar cells characterization by EIS

To better understand the photovoltaic behaviour of the different DSCs and correlate it with the electrolyte's composition, the recombination dynamics of the cells were explored via EIS[54]. The spectra (not shown) typically exhibited three prominent semicircles, presenting the classical behaviour, for standard iodine-based electrolyte cells[55]. The equivalent circuit used to fit the spectra was similar to the one utilized for the symmetrical cells by simply adding in series an extra *RC* circuit, which appeared at intermediate frequencies, representing the TiO_2/electrolyte interface. Here, we focused on the charge recombination resistance at the TiO_2/electrolyte interface (R_{rec}) and the chemical capacitance (C_μ) that stands for the change of the electron density as a function of the Fermi level[56].
An interesting feature is that there was a distinctive difference between the results obtained for electrolytes C1 and C2, whose major components are ionic liquids 1-ethyl-3methylimidazolioum iodide and 1,3-dimethylimidazolium iodide, which are solid in room temperature and become liquid after heating or after blending with a liquid at room temperature non iodide ionic liquid, and the results obtained with electrolytes C3,C4 and C6, where all ionic liquids used are in the liquid state at room temperature.

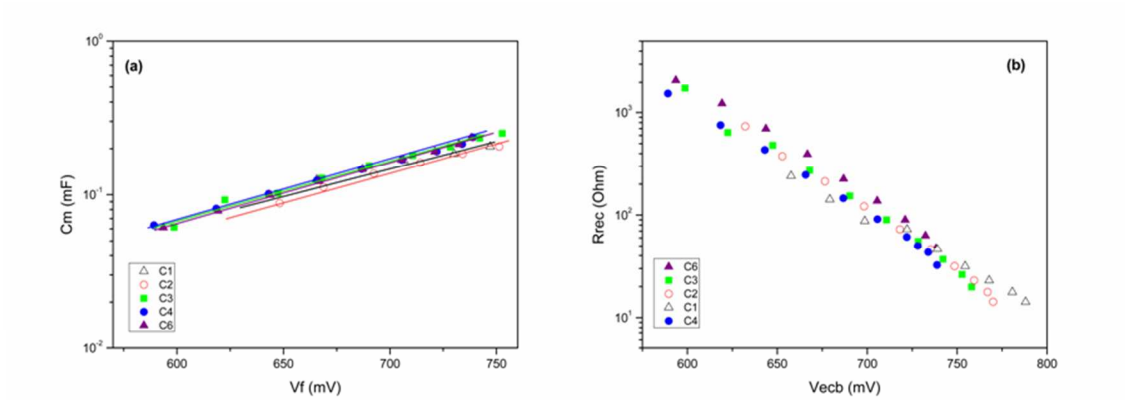

Fig. 5 Chemical capacitance (C_μ) of the TiO_2 semiconductor plotted against the actual potential of the photoelectrode V_F (a) and recombination resistance (R_{rec}) plotted against the voltage at the equivalent band position V_{ecb} (b) for DSCs using redox electrolytes based on $[C_nC_1im]I$/EMimDCA double salt ILs.

The chemical capacitance was estimated through fitting and plotted (Fig. 5a) against the actual voltage drop in the photoelectrode (denoted as V_F); V_F was estimated as $V_F = V_{applied} - V_{series}$, where V_F is the corrected voltage, $V_{applied}$ is the applied voltage during the measurement and V_{series} is the voltage drop at the total series resistance R_{series}[57]. The chemical capacitance showed, as expected, an exponential behaviour confirming the exponential trap energy distribution below the conduction band edge[58]. If we assume that all cells have similar trap distributions (since they use the same TiO_2 working electrode), the observed shifts can be attributed to shifts in the conduction band edge (E_c)[59]. The small E_c shifts, observed by varying the alkyl chain of the $[C_nC_1im]I$ ionic liquid, could be explained by the different dipole moments of the five different organic salts, affecting the charge of the TiO_2 surface upon contact with the electrolyte. Taking as reference the energy of the conduction band edge for the C6 electrolyte-based DSC and shifting the (C_m-V_F) curves of the other 4 electrolytes-based DSCs (Fig. 5a), we could draw R_{rec} against V_{ecb} (Fig. 5b) that is the voltage at the equivalent band position[54]. Thereby, we were able to directly compare the recombination resistances of the DSCs independently of conduction band edge shifts. It was then evidenced that the recombination rates of all cells were similar and the slight differences in their V_{oc} values could be assigned to small E_c shift towards negative potentials for the C2 and C1 electrolyte (16 and 8 mV respectively), while we receive identical results for electrolytes C3,C4 and C6, presenting no shift. High recombination rates were expected for all electrolytes under study, bearing in mind that ILs are characterized by large reorganization energy, related to the non-favourable chemical environment that ILs provide to the active species of the electrolytes, e.g. strong interaction between ions and solvent molecules. This leads to wider distribution of acceptor states that multiplies the number of recombination routes for photogenerated electrons.[60] All electrolytes present very similar recombination rates, suggesting that the length of alkyl chain of the imidazolium iodide ionic liquid has no significant effect on the recombination dynamics.
It must pointed out that the use of $[C_nC_1im]I$/EMimDCA double salt ILs influenced not only the overall power conversion efficiency and electrical parameters of the corresponding DSCs, but also led to DSCs with enhanced V_{oc}, fact justified by the high chemical capacitance

Journal of Materials Chemistry A Accepted Manuscript

values obtained through exploration of the electron dynamics of the solar cells via electrochemical impedance spectroscopy.

4. Conclusions

New redox active electrolytes were prepared using double salt ionic liquids based on mixtures of $[C_nC_1im]I$ with EMimDCA, incorporating the iodide/triodide mediator. A systematic exploration of the effect of the alkyl chain length of the $[C_nC_1im]I$ component on the physicochemical properties in the corresponding blends with 1-ethyl-3-methyl imidazolium dicyanamide and on their photovoltaic performance upon incorporation in dye solar cells was performed. Density and viscosity measurements as a function of temperature revealed that the viscosity of the electrolyte blends followed the classical Vogel-Tammann-Fulcher (VTF) law. Linear sweep voltammetry and electrochemical impedance spectroscopy experiments have proven that both diffusion and conductivity decreased with increasing viscosity for electrolytes C3-C6, even though charge transport did not follow a Stokesian behaviour as other standard liquid conductors, due to the activation of the Grotthus-like exchange mechanism in ionic liquids.The same trend was not observed for electrolytes C1 and C2, which are the ones incorporating ionic liquids that are solid in room temperature and become liquid after being blended with the non iodide ionic liquid,or after heating. These two systems have no obvious trend in terms of viscosity and density as a function of temperature either. The increase of the alkyl chain of the CnC1im constituent results in a net reduction of the density and concomitant increase of the viscosity of the corresponding electrolytes based in the [CnC1im]I / EMimDCA mixtures (no linear behavior). It has been proved that EMimDCA IL is excellent solvent for both solid and liquid [CnC1im]I materials, giving electrolytes with density and viscosity values significantly lower than those based the [CnC1im]TCM//PMII mixtures[29]. In addition to their lower viscosity, the new electrolytes based on the [CnC1im]I/EMimDCA double salt ILs present significantly higher values for the diffusion coefficient of triiodides (DI3-), lower series resistance (Rs) and higher conductivity (κ). Moreover, we have demonstrated that the alkyl chain length of the $[C_nC_1im]$ constituent in the $[C_nC_1im]I$/EMimDCA blend influenced the overall power conversion efficiency and electrical parameters of the corresponding DSCs. The best performance was observed for cells based on the C_1mimI blend, where the power conversion efficiency (PCE) reached 5.53 %, with minor difference from C_2mimI, whose efficiency reached 5.27%, possibly owing to their similar conductivity. The efficiencies further increased up to 6.5% at low light intensity, when the cells were illuminated by 0.1 sun. The use of the new electrolytes leads to DSCs with enhanced V_{oc}, fact justified by the high chemical capacitance values obtained through exploration of the electron dynamics of the solar cells via electrochemical impedance spectroscopy. Variations in the fill factor were attributed to differences in the resistances at the Pt/electrolyte interface. These variations are the main cause of differences at the overall power efficiency of the solar cells. Although the performance of ionic liquids in DSCs (as compared with standard organic solvent electrolytes) is controlled by mass transport limitation however, recombination in DSCS based on ionic liquids is an intrinsic problem, due to their polar nature and must also be taken into account. The reported results prove the high potential of the ionic liquid blends and pave novel roads towards further optimization and practical applications of these materials in industrial solar energy conversion devices (namely dye-sensitized solar cells) and other energy-related applications. Work is currently in progress aiming to optimize the device performance by combining the new DSIL based redox electrolytes with innovative light harvesting molecular dyes [matching better the solar spectrum and presenting higher (than Z907) molar extinction coefficient values] and thinner high quality mesoporous semiconducting titania films (avoiding charge recombination and permitting faster and more efficient charge collection yields).

Acknowledgements

The research leading to these results has received funding from the European Union Seventh Framework Programme [FP7] under grant agreement 316494 (DESTINY) project. Additional financial support is also acknowledged by the European Social Fund and Greek national funds through ARISTEIA (AdMatDSC-1847) operational research programs.

Notes and references

[a] *Institute of Advanced Materials, Physicochemical Processes, Nanotechnology and Microsystems (IAMPPNM), Division of Physical Chemistry, National Center for Scientific Research "Demokritos", 153 10 Aghia Paraskevi Attikis, Athens, Greece. E-mail: papi@chem.demokritos.gr; Tel : +30-2106503644; Fax : +30-2106511766.*

1 B. O' Regan, M. Gratzel, *Nature*, 1991, **353**, 737.
2 M. Gratzel, *Nature*, 2001, **414**, 338.
3 M. Gratzel *Inorg. Chem*., 2005, **44**, 6841.
4 T. Stergiopoulos, A. G. Kontos, V. Likodimos, D. Perganti and P. Falaras , *J. Phys. Chem. C*, 2011, **115**, 10236.
5 (a) Q. Yu, Y.Wang, Z.Yi, N.Zu, J.Zhang, P.Wang, *ACS Nano*, 2010, **4**, 6032 (b) S. Mathew, A. Yella, P. Gao, R. Humphry-Baker, B. F.E. Curchod, N. Ashari-Astani, I. Tavernelli, U. Rothlisberger, M.K Nazeeruddin, M. Grätzel, *Nature Chem.*, 2014, **6**, 242.
6 T. Welton, *Chem Rev*. 1999, **99**, 2071.
7 R.D.Rogers, K.R.Seddon, S.Volkov,Eds., *Green Industrial Applications of Ionic Liquids, Kulwer Academic Press* 2003.
8 P. Wasserscheid, T. Welton, *Ionic Liquids in Synthesis, Wiley-VCH,* Weinheim, Germany 2003.
9 P. Dyson, *Transition Met. Chem* 2002, **27**, 353.

Journal of Materials Chemistry A Accepted Manuscript

10 H. Xue, J. M. Shreeve, *Eur. J. Inorg. Chem*. 2005, 2573.
11 S.Kambe, S.Nakade, T.Kitamura, Y.Wada, S.Yanagida, *J. Phys .Chem. B* , 2002, **106**, 2967.
12 F.Zhaofu, T. J. Geldbach, D. B. Zhao, P. J. Dyson, *Chem. – Eur. J*. 2006, **12**, 2122.
13 N.Kopidakis, N.R.Neale, A.J.Frank, *J. Phys. Chem. B* , 2006, **110**, 12485.
14 H.Kusama, H.Orita, H.Sugihara, *Langmuir* 2008, **24**, 4411.
15 D.F.watson, G.Meyer, *J. Coord. Chem. Rev*. 2004, **248**, 1391.
16 K.M.Son, M.G.Kang, R.Vittal, J.Lee, K.J.Kim, *J. Appl.Electrochem*. 2008, **38**, 1647.
17 T.Y.Cho, S.G.Yoon, S.S.Sekhon, C.H.Han, *Bull. Korean Chem. Soc.,* 2011, **32** , 2058.
18 C.Xi, Y.Cao, Y.Cheng, M.Wang, S.M.Zakeeeruddin, M.Gratzel, P.Wang, *J. Phys. Chem. C* 2008, **112**, 11063.
19 R.Hagiwara,Y.Ito, *J. Fluorine Chem.* 2000, **105**, 221.
20 T.Nishida, Y.Tashiro, M.Yamamoto, *J. Fluorine Chem*. 2003, **120**, 135.
21 M. Gorlov, L. Kloo, Dalton Trans., 2008, 2655.
22 Y. Bai, Y. Cao, J. Zhang, M. Wang, R. Li, P. Wang, S. M. Zakeeruddin, M. Grätzel, *Nature Mater.*, 2008, **7**, 626.
23 F.Hao, Y.Lin, G.Yang, G.Wang, J.Li, *Electrochim. Acta.*, 2011, **56**, 5605.
24 J.D.Holbrey, K.R. Seddon, K. R. *J. Chem.Soc., Dalton Trans*. 1999, 2133.
25 P.Cheng, W.Wang, T.Lan, R.Chen, J.Wang, J.Yu, H.Wu, H.Yang, C.Deng, S.Guo, *J. Photochem. Photobiol., A*, 2010, **2012**, 147.
26 D.Kuang, C.Klein, Z.Zhang, S.Ito, J.E.Moser, S.M.Zakeeruddin, M.Grätzel, *small*, 2007, **3** , 2094.
27 P.Wang, S.M.Zakeeruddin, R.Humphry-Baker, M.Grätzel , *Chem.Mater.*, 2004, **16**, 2694.
28 D.Kuang, P.Wang, S.Ito, S.M.Zakeeruddin, M. Grätzel, *J. Am. Chem. Soc. ,* 2006, **128**, 7732.
29 G. Chatel, J. F. B. Pereira, V. Debbeti, H. Wang, R. D. Rogers, *Green Chem*., 2014, **16**, 2051.
30 M.Bidikoudi, T.Stergiopoulos, V.Likodimos, G.E.Romanos, M.Fransisco, B.Iliev, D.Adamova, T.Schubert, P.Falaras, *J. Mater. Chem. A***,** 2013,**1**, 10474.
31 M. Dürr, A. Yasuda, G. Nelles, *Appl. Phys.Lett.*, 2006, **89**, 061110.
32 H. J. Snaith, *Nature Photon.,* 2012, **6**, 337.
33 H. Niedermeyer, J. P. Hallett, I. J. Villar-Garcia, P. A. Hunt, T. Welton, *Chem. Soc. Rev.,* 2012, **41**, 7780.
34 K. Kalyanasundaram , Dye Sensitized solar cells , *Fundamental Sciences Chemistry*, EPFL Press, 2010.
35 William M. Haynes CRC Handbook of Chemistry and Physics, 93rd Edition, *Science* , 2012.
36 N. Papageorgiou, Y. Athanassov, M. Armand, P. Bonhote, H. Petterson, A. Azam, M. Griitzel, *J. Electrochem. Soc.*, 1996, **143**, 3099.
37 D. R. MacFarlane, S. A. Forsyth, J. Golding, G. B. Deacon, *Green Chemistry*, 2002, **4**, 444.
38 D. Xiao, J. R. Rajian, L. G. Hines, S. Li, R. A. Bartsch, E. L. Quitevis, *J. Phys. Chem. B,* 2008, **112**, 13316.
39 Y. Wu, L. Hao, C.-W. Kuo, Y.-C. Lin, S.-G. Su, P.-L. Kuo, I-W. Sun, *International Journal of Electrochemical Science*, 2012, **7**, 2047.
40 K.R. Seddon, A.S. Starck, M.J. Torres, ACS Symposium Series 901, Washington, DC, 2004.
41 (a) I. Krossing, J.M. Slattery, C. Daguenet, P.J. Dyson, A. Oleinikova, H. Weingärtner, *J. Am. Chem. Soc.*, 2006, **128**, 13427. (b) T. Köddermann, D. Paschek, R. Ludwig, *ChemPhysChem*, 2007, **8**, 2464.
42 F. Hao and H. Lin, *RSC Adv.,* 2013,**3**, 23521.
43 A. Hauch and A. Georg, *Electrochim. Acta*, 2001, **46**, 3457.
44 (a) P. Wachter, C. Schreiner, M. Zistler, D. Gerhard, P. Wasserscheid, H. J. Gores, *Microchim. Acta*, 2008, **160**, 125; (b) M. Zistler, P. Wachter, C. Schreiner, H. J. Gores, *J. Mol. Liq.* 2010, **156**, 52.
45 J. D. Roy-Mayhew, G. Boschloo, A. Hagfeldt and I. A. Aksay, *ACS Appl. Mater. Interf.,* 2012, **4**, 2794.
46 T. Stergiopoulos, M. Bidikoudi, V. Likodimos and P. Falaras, *J. Mater. Chem.,* 2012, **22**, 24430.
47 S. –J. Seo, S. –H. Yun, J. –J. Woo, D. –W. Park, M. –S. Kang, A. Hinsch and S. –H. Moon, *Electrochem. Commun.,* 2011, **13**, 1391.
48 P. Wachter, M. Zistler, C. Schreiner, M. Fleischmann, D. Gerhard, P. Wasserscheid, J. Barthel and H. J. Gores, *J. Chem. Eng. Data*, 2009, **54**, 491.
49 M. Zistler, P. Wachter, P. Wasserscheid, D. Gerhard, A. Hinsch, R. Sastrawan and H. J. Gores, *Electrochim. Acta,* 2006, **52**, 161.
50 P. Wang, B. Wenger, R. Humphrey-Baker, J.-E. Moser, J. Teuscher, W. Kantlehner, J. Mezger, E. V. Stoyanov, S. M. Zakeeruddin and M. Grätzel, *J. Am. Chem. Soc.,* 2005, **127**, 6850.
51 M. Liberatore, A.Petrocco, F. Caprioli, C. La Mesa, F. Decker and C. A. Bignozzi, *Electrochim. Acta*, 2010, **55**, 4025.
52 J.R. Jennings, Y. Liu, Q. Wang, S.M. Zakeeruddin, M. Grätzel, *Phys. Chem. Chem. Phys*., 2011, **13**, 6637.
53 M. Konstantakou, P. Falaras, T. Stergiopoulos, *Polyhedron,* 2014, **In Press**, DOI information: 10.1016/j.poly.2014.05.011
54 F. Fabregat-Santiago, G. Garcia-Belmonte, I. Mora-Seró and J. Bisquert, *Phys. Chem. Chem. Phys.,* 2011, **13**, 9083.
55 Q. Wang, S. Ito, M. Grätzel, F. Fabregat-Santiago, I. Mora-Seró, J. Bisquert, T. Bessho and H. Imai, *J. Phys. Chem. B,* 2006, **110**, 19406.
56 S. R. Raga, E. M. Barea and F. Fabregat-Santiago, *J. Phys. Chem. Lett.,* 2012, **3**, 1629.
57 F. Fabregat-Santiago, J. Bisquert, E. Palomares, L. Otero, D. Kuang, S. M. Zakeeruddin and M. Grätzel, *J. Phys. Chem. C,* 2007, **111**, 6550.
58 J. Bisquert, *Phys. Chem. Chem. Phys.,* 2003, **5**, 5360.
59 V. Pedro-González, X. Xu, I. Mora-Seró and J. Bisquert, *ACS Nano,* 2010, **4**, 5783.
60 J. Idigoras, L. Pelleja,E. Palomares, J.A Anta, *J. Phys. Chem. C,* 2014, **118**, 3878.

Journal of Materials Chemistry A Accepted Manuscript

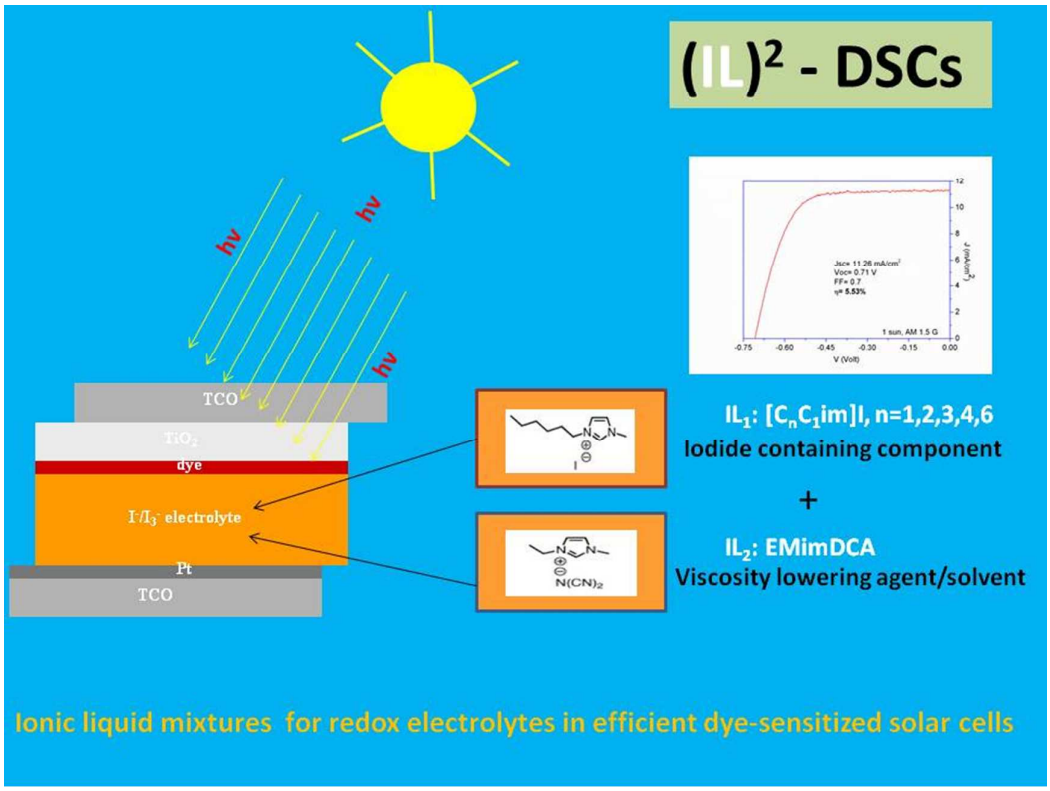

[CnC_1im]I/EMimDCA double salt Ionic liquid mixtures presenting low viscosity and high conductivity were used for the preparation of redox active electrolytes that were successfully incorporated in highly efficient dye-sensitized solar cells

Journal of Materials Chemistry A Accepted Manuscript